Adsorption State and Morphology of Tetracyanoquinodimethane Deposited from Solution onto the Atomically Smooth Native Oxide Surface of Al(111) Films Studied by X-ray Photoelectron Spectroscopy and Atomic Force Microscopy

Morihide Higo,* Tadanobu Futagawa, Masaru Mitsushio, Toshifumi Yoshidome, and Yoshihisa Ozono†

Department of Applied Chemistry and Chemical Engineering, Faculty of Engineering, Kagoshima University, 1-21-40, Korimoto, Kagoshima 890-0065, Japan

Received: January 31, 2003; In Final Form: April 20, 2003

The adsorption state and morphology of tetracyanoquinodimethane (TCNQ) deposited from acetonitrile solutions onto atomically smooth native oxide surfaces of Al(111) films were investigated by X-ray photoelectron spectroscopy (XPS) and atomic force microscopy (AFM). The analysis of the XP spectra of the deposited TCNQ showed that it is adsorbed as both a neutral and ionized state on the surfaces and the intensity for the former increases more rapidly than that for the latter as the concentration increases. The atomically smooth surfaces of the Al films allowed the detailed observation and analysis of the morphology of the deposited TCNQ. The surface height analysis (bearing analysis) of the AFM images of the deposited TCNQ showed that it is adsorbed as both a uniform film on a nanometer scale and micrometer-sized particles with height ranging from 10 to 100 nm above the surfaces. The volumes of the thin uniform film and the large particles of the deposited TCNQ could be obtained separately from the analysis of the bearing histograms and bearing area curves of the AFM images. A similarity in the dependence of both the volumes of the large and small particles of the deposited TCNQ obtained by AFM and in that of the surface concentrations of neutral and ionized TCNQ obtained by XPS on the concentration of TCNQ in solution clarified the adsorption mechanism. It is concluded that the large particles are identified as microcrystallites of neutral TCNQ and the thin uniform film results predominantly from corrosion of the oxide surface by the TCNQ anion formation reaction.

Introduction

7,7,8,8-Tetracyanoquinodimethane(TCNQ) which has 4 cyano groups and delocalized π electrons is a strong electron acceptor and forms a variety of charge-transfer complexes with inorganic and organic donors.[1−4] Some complexes of TCNQ and its derivatives exhibit unique electrical and optical field-induced switching and memory phenomena.[5−18] The resistivity of Cu−TCNQ or Ag−TCNQ complex films grown on Cu or Ag and coated with Al films switches from a high impedance state to a low impedance state under the application of an external electric field or laser irradiation. These materials have been proposed for applications in molecular electronic devices such as switches and data storage media.[5−18] However, the mechanism of the resistivity transition in the switching device and the resulting structure change of the TCNQ complexes are not well understood. A detailed understanding of the morphology, spectroscopy, and chemistry of these materials in bulk, in thin films, at interfaces, and at surfaces is necessary, because the electric, magnetic, and optical properties of these molecular semiconductors vary greatly with crystallographic orientation, degree of crystallinity, and surface orientation of the films.[1−4]

Morphological studies of TCNQ and its metal complexes have been made by scanning electron microscopy (SEM), scanning tunneling microscopy (STM), and atomic force microscopy (AFM).[19−29] Yamaguchi et al.[19,24,25] imaged the surface structures of Ag−TCNQ and Cu−TCNQ films on graphite (HOPG) with molecular level resolution by STM. They also observed a field-induced charge-transfer reaction driven by the electric field generated by the microscope tip potential when the bias voltage exceeds the switching threshold of the metal−TCNQ complexes. Similar observations were reported for Cu−TCNQ films on HOPG by Matsumoto et al.[20] Hietschold et al.[21] applied both AFM and STM to image polycrystalline TCNQ films on a steel substrate used as a pressure sensor. Hoagland et al.[22] used SEM and STM to determine the morphology of Cu−TCNQ films made using solution-phase and vapor-phase spontaneous reaction methods. They showed that all the films display roughness on the order of the film thickness and that the morphology of the films varied significantly with the preparation procedure. Gu et al.[23] observed many nanometer-sized passageways in the growth direction in the crystalline grains of Cu−TCNQ films prepared by the spontaneous reaction method using AFM. Gao et al.[26] used STM to observe a periodic arrangement in thin films prepared on HOPG by an ionized-cluster-beam deposition method and interpreted it as molecular chains of TCNQ. Kamna et al.[27] also observed molecular chains of TCNQ along the steps of Cu(111) at low surface coverage and at 77 K by STM. Heintz et al.[28] reported two distinct polymorphs of Cu−TCNQ in the films synthesized via solution reactions of Cu(I) precursors with anions of TCNQ or by direct redox reactions of Cu(0) with neutral TCNQ using SEM and X-ray diffraction. Lijun and Itaya[29] found a highly ordered long-range adlayer of TCNQ on

* Author to whom correspondence should be addressed. Fax: +81-99-285-8344. E-mail: higo@apc.kagoshima-u.ac.jp.

† Center for Instrumental Analysis, Kagoshima University, 1-21-30, Korimoto, Kagoshima 890-0065, Japan.

10.1021/jp0301352 CCC: $25.00
Published on Web 05/24/2003

a Cu(111) electrode in $HClO_4$ solution by in situ STM. They concluded that TCNQ is adsorbed on the surface in flat-lying orientation.

X-ray photoelectron spectroscopy (XPS) spectra of TCNQ and its complexes have been measured and studied.[30−50] Ikemoto et al.[30−33] studied TCNQ and its complexes and reported that satellites appear 2 to 4 eV on the higher-binding energy side of both the N1s and C1s main peaks. They concluded that the satellites are attributed to a shake-up process involving intramolecular transitions between the π-electron valence molecular orbitals in both neutral and ionic TCNQ species. The satellites were also observed in the N1s spectra of TCNQ and its complexes by many researchers.[34−45] High-resolution XPS spectra of C1s and N1s of TCNQ and Cu−, Ni−, and Li− complexes were measured by Lindquist and Hemminger.[40,41] The growth of TCNQ films on Ni(111) from the gas phase was investigated by Giergiel et al.[43,44] They reported that TCNQ forms stable multilayer films at room temperature in which both reacted monoanionic and unreacted neutral TCNQ are present. Patterson et al.[45] reported the characterization of TCNQ films on Cu, Au, Pt, and SnS_2 and found TCNQ reduction in the multilayer films. Arena et al.[46,47,49] studied spectroscopic and electronic properties of Cu−TCNQ and Ag−TCNQ dissolved into a polymeric matrix, Cd−TCNQ synthesized via an electrochemical process, and Ag−phen−TCNQ obtained by a charge-transfer reaction of Ag, TCNQ, and 1,10-phenanthroline (phen). Iwamoto et al.[48] studied the adsorption of TCNQ from solutions on oxidized Al films and reported the predominance of neutral TCNQ on the surfaces. Long and Willett[50] synthesized two new Ni complexes of TCNQ by an electroplating technique and studied the magnetic properties. They reported that the oxidation states of TCNQ are stabilized by control of the applied electroplating voltage.

The vibrational spectra of TCNQ and its derivatives adsorbed on alumina have been recorded and studied by inelastic electron tunneling spectroscopy (IETS).[51−54] Coleman et al.[51,52] compared the tunneling spectra of TCNQ adsorbed on alumina with the infrared and Raman spectra of the neutral TCNQ and of the $TCNQ^{-1}$ and concluded that the monoanion of TCNQ is the stable form on alumina. Cooper et al.[53] compared the tunneling spectrum of TCNQ on alumina with the vibrational structure in the optical reflectivity of K−TCNQ and found a good correspondence between these results. Hipps and Mazur[54] measured the tunneling spectra of TCNQ on alumina doped under inert conditions using a glovebox deposition system. They reported that the surface species formed are independent of the presence of air during the adsorption step and concluded that TCNQ is adsorbed as the monoanion on the alumina surfaces. These tunneling spectra show that the monoanion of TCNQ is the dominant surface species on alumina. However, our early XPS study[48] of TCNQ adsorbed on an oxidized Al film suggested that neutral TCNQ predominates on the alumina surface. This difference in results could be due to the morphology of the adsorbed TCNQ, because TCNQ is adsorbed from monolayer to multilayer coverage on the alumina surfaces, and IETS is sensitive only to areas having sub- to two monolayer coverage.[51−54] On the other hand, XPS probes all the material within a few tens of nanometers of the surface. The vibrational spectra of TCNQ adsorbed on a Cu(111) single-crystal surface at 100 K have been obtained using high-resolution electron energy loss spectroscopy (HREELS) by Erley and Ibach.[55] They found that TCNQ is adsorbed predominantly as the trianion with its plane parallel to the surface for coverage up to a single monolayer. As the coverage increases, the monoanion was dominant in the second layer and finally neutral TCNQ appeared in the multilayer.

These electron spectroscopies have shown that TCNQ interacts with metals and aluminum oxide to produce a surface anionic species. Neutral TCNQ is also present in multilayer films. Although these electron spectroscopies provide information about the adsorption state of TCNQ, the morphology of the adsorbed TCNQ at low coverage and the degree of surface roughness have not been considered. Morphological observations of TCNQ at low coverage on reactive surfaces are needed in order to understand thoroughly the adsorption chemistry of this important redox active species and to provide a model for the adsorption.

We have reported the preparation and characterization of very smooth Al films on a nanometer scale over a wide surface area.[56,57] Such atomically smooth films are important and useful in modern surface science techniques in order to study adsorption from submonolayer to multilayer coverage.[58−61] The atomically smooth Al films enabled us to observe the morphology of TCNQ deposited from various solutions onto the oxidized surfaces.[59−61] The analysis of the AFM images showed that TCNQ is adsorbed onto the surfaces as both a uniform film on a nanometer scale and micrometer-sized particles with many morphologies.[59−61] We have demonstrated that these atomically smooth Al films are very useful for the detailed characterization and morphological observation of TCNQ on alumina in our preliminary study.[60] In the present paper, we report a thorough XPS and AFM study of the adsorption of TCNQ deposited from acetonitrile solutions onto atomically smooth native oxide surfaces grown on polycrystalline Al(111). We also demonstrate the usefulness of the combination of XPS and AFM using these atomically smooth Al films as the substrate to study the adsorption mechanism.

Experimental Section

Atomically smooth Al films with a thickness of 150 nm were prepared by vacuum evaporation as reported previously.[56,57] Aluminum (99.999%) was evaporated from a molybdenum boat onto previously cleaved and heated (550 °C) mica substrates (9×12 mm^2) at a temperature of 350 °C and at a pressure of $(1.5-1.9) \times 10^{-6}$ Torr (1 Torr = 133.322 Pa) in a metal bell-jar evaporator equipped with a liquid-nitrogen-trapped 6-in. diffusion-pump. The temperature was measured with an iron−constantan thermocouple. The prepared Al films were cooled to below 90 °C in the vacuum and moved into another bell-jar evaporator equipped with a liquid-nitrogen-trapped 4-in. diffusion-pump. The surfaces of the Al films were oxidized in an oxygen dc glow discharge (75 mTorr, 5 mA, 30 s) to form a stable surface oxide. The root-mean-square roughness (Rms) of a 1×1-μm^2 area of the atomically smooth Al film used was 0.42 ± 0.16 nm.

TCNQ (Tokyo Kasei, powder, >98%) was deposited onto the surfaces of the atomically smooth oxidized Al films with various concentrations (0.04−1.03 mg mL^{-1}) of acetonitrile solutions at a room temperature (14−25 °C) and at a humidity of 51−68% by a spin doping technique.[59−61] After the spinning, the doped oxidized Al film was returned to the vacuum chamber and pumped at a pressure of 10^{-5} Torr for 5 min to remove volatile materials.

The XP spectra of the adsorbed TCNQ on the atomically smooth oxidized Al films and the TCNQ powder on a conductive tape were measured with a Shimadzu ESCA-1000 and Mg Kα radiation (1253.6 eV) excitation. Photoelectrons emitted normal to the surface (3×10 mm^2) were analyzed with

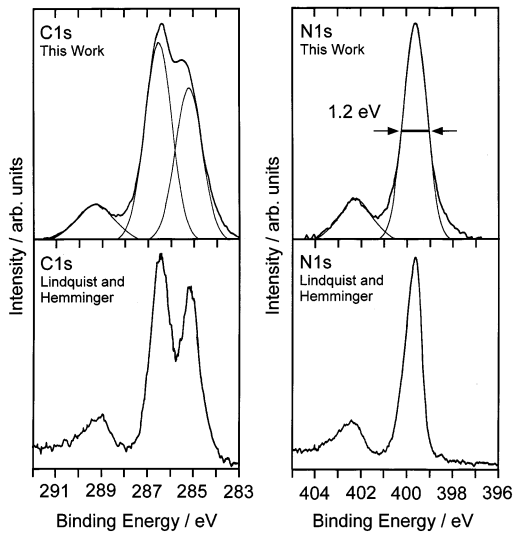

Figure 1. XP spectra of C 1s and N 1s of TCNQ powder. The line shape of the spectrum was deconvoluted with a Gaussian shape. The full width at half-maximum of the N 1s line at 399.7 eV is 1.2 eV. The spectra measured at a higher resolution by Lindquist and Hemminger[40,41] are also shown for comparison.

a data collection interval of 0.1 eV with the analyzer pass energy set at 15.75 eV. The resolution was estimated to be 1.1 eV from the peak width of the Ag $3d_{5/2}$ line at 368.3 eV. The binding energy was calibrated to the C 1s line of the surface at 285.0 eV.

The AFM images (256 pixels wide) of the adsorbed TCNQ were taken with a Digital Instruments NanoScope III operating in contact mode in air. The cantilever was 200-μm long Si_3N_4 with a force constant of 0.06 N/m. The images were automatically plane-fitted to account for sample tilt.

Results and Discussion

XP Spectra of TCNQ on Atomically Smooth Oxidized Al Films. The XP spectra of TCNQ powder over the regions of C 1s and N 1s are shown in Figure 1 with those obtained by Lindquist and Hemminger[40,41] using a higher resolution. A Gaussian shape was used to deconvolute the peaks of our spectra. The C 1s spectrum of the powder has three peaks at 285.3, 286.6, and 289.2 eV, and these peaks are assigned to the C 1s of the ring, wings including the cyano groups, and the shake-up satellite of neutral TCNQ ($TCNQ^0$), respectively.[40,41] The first peak is smaller than the second peak by about 12% and X-ray sensitive.[40] The satellite peak is common to core level spectra of TCNQ and attributed to an intramolecular electronic excitation process.[30−45] It arises from the emission of a 1s electron accompanied by the excitation of an electron in the highest occupied molecular orbital (HOMO) of TCNQ to the lowest unoccupied molecular orbital (LUMO) of the photoion.[30−33,40,41] The satellite peak is only associated with the C1s peak at 286.6 eV, suggesting that the HOMO and LUMO of TCNQ are located near the cyano ends of the molecle.[40,41] The N 1s spectrum of the powder has two peaks at 399.7 and 402.3 eV, and these peaks are due to the N 1s of the cyano groups and the shake-up satellite of $TCNQ^0$, respectively.[40,41] The intensity of the satellite peak is 20−30% of that of the main peak.[33,40,42] The main peak in the spectra of metal complexes is shifted up to 1 eV to lower binding energy relative to that of $TCNQ^0$.[31,32,35−37,41] The satellite peaks in these spectra appear in varying intensity and in different energies; the separation from the main peak in the spectra of LiTCNQ, $Ni(TCNQ)_2$, and CuTCNQ is 2.6, 2.4, and 1.4 eV, respectively.[41] The full width at half-maximum of the N 1s main peak in our spectrum of $TCNQ^0$ is 1.2 eV. The XP spectra of the TCNQ powder show that the peak positions and relative intensities of these deconvoluted peaks agreed well with those of the peaks of the high-resolution spectra.[40,41] These results show that the sample of TCNQ used and the measurements are appropriate for obtaining a good XP spectrum of TCNQ.

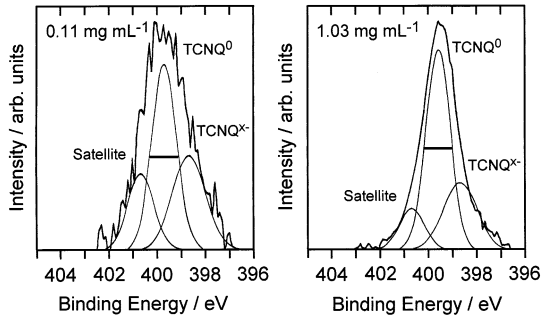

Figure 2. XP spectra of N 1s of TCNQ deposited on the atomically smooth oxidized Al films from CH_3CN solutions of 0.11 and 1.03 mg mL^{-1}. The line shape was deconvoluted into three peaks of the satellite, neutral, and anionic TCNQ. The full width at half-maximum of the deconvoluted N 1s line for $TCNQ^0$ near 400 eV is 1.2 eV.

The XP spectra of TCNQ deposited on atomically smooth oxidized Al films from CH_3CN solutions of 0.11 and 1.03 mg mL^{-1} are shown in Figure 2. The peak width of the adsorbed TCNQ on the surface is larger than 1.2 eV and becomes wider for the spectra obtained from lower concentrations. The peak was deconvoluted into three peaks. The main peak near 400 eV (399.6−400.0 eV) is due to $TCNQ^0$ and was deconvoluted using a peak width of 1.2 eV. The peak near 399 eV (398.6−398.8 eV) has a chemical shift of about 1 eV and is assigned to ionized TCNQ ($TCNQ^{x-}$) formed from interaction with the oxide surface.[48,60] Though the peak width is wider than that of $TCNQ^0$, suggesting more than one anionic state may contribute to this peak, the detailed anionic state is not clear because the amount of the peak shift (about 1 eV) is equal to that of the resolution used. The satellite peak associated with both $TCNQ^0$ and $TCNQ^{x-}$ lies near 401 eV (400.7−401.1 eV); its separation from the neutral peak becomes smaller than that (2.6 eV) of the neutral TCNQ powder, because of the implication of the satellite peak of $TCNQ^{x-}$ at lower energies. The relative intensity of the satellite peak to the total intensity of $TCNQ^0$ and $TCNQ^{x-}$ ranges from 16 to 30%. The XP spectra of the deposited TCNQ on the atomically smooth oxidized Al films from acetonitrile solutions show that it is adsorbed as both the neutral and anionic state on the surfaces. The coexistence of neutral and anionic TCNQ in the multiplayer films deposited from the gas phase on Ni, Cu, Au, and Pt surfaces has been reported by XPS[43−45] and HREELS.[55] The monoanion is present on Ni,[43,44] Au, and Pt;[45] on the other hand, the trianion and monoanion were found on Cu.[55]

The peak intensities (peak areas) of the N 1s spectra of $TCNQ^0$ and $TCNQ^{x-}$ on the atomically smooth oxidized Al films doped from various concentrations of CH_3CN solutions were measured and the result is shown in Figure 3. The uncertainty for the intensity of $TCNQ^{x-}$ is mainly caused by a random experimental error and estimated to be about 20%. The intensity of $TCNQ^0$ has the uncertainty of about 18% caused by both a random experimental error (about 10%) and the uncertainties from the contribution of the satellite and $TCNQ^{x-}$ (less than 15%). The intensities of both the species on the surfaces doped from lower concentrations are weak and almost

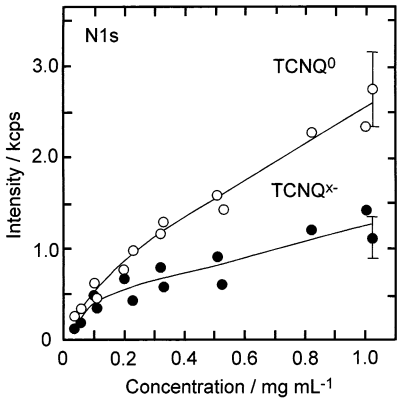

Figure 3. Intensities of the N 1s lines of neutral and anionic TCNQ of the TCNQ-deposited atomically smooth oxidized Al films from various concentrations of CH_3CN solutions. Uncertainties for the intensities of $TCNQ^0$ and $TCNQ^{x-}$ are 18 and 20%, respectively.

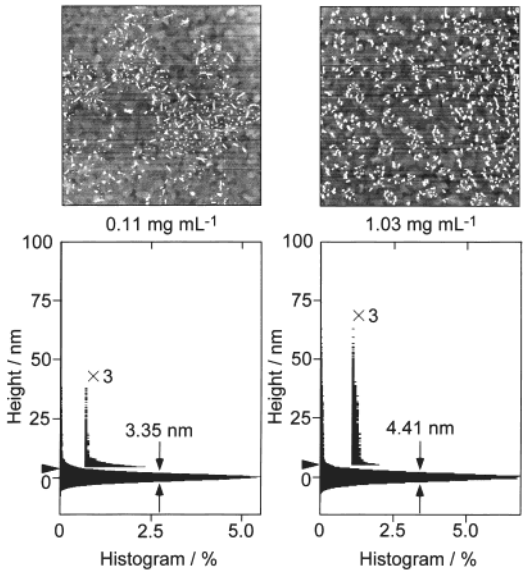

Figure 4. AFM top views (top) and bearing histograms (bottom) of the TCNQ-deposited atomically smooth oxidized Al films from CH_3CN solutions of 0.11 and 1.03 mg mL^{-1}. Image size: 30 μm wide and 100 nm gray scale. The bearing histogram of the TCNQ-deposited oxidized Al film shows a bimodal height distribution of TCNQ particles. The bearing volumes of large and small TCNQ particles are separated from that of total TCNQ particles at a height (indicated by the marker) of the bearing width (W) in the histogram.

equal. The intensity of $TCNQ^{x-}$ increases slowly with the concentration. On the other hand, the intensity of $TCNQ^0$ increases rapidly with the concentration and becomes two to three times larger than that of $TCNQ^{x-}$ at 1.0 mg mL^{-1}. The result of XPS shows that the quantities of the neutral and anionic TCNQ deposited on the oxidized Al films strongly depend on the solution concentration used. However, detailed chemical states and the adsorption mechanism of TCNQ on the surfaces are not clear only from these XPS results.

Morphology of TCNQ on Atomically Smooth Oxidized Al Films. The morphology of the deposited TCNQ on the surfaces was observed by AFM after the XPS measurements. The observation and bearing analysis were made on four randomly selected places in a sample and the results of the analysis were averaged. Typical examples of the images and their bearing histograms are shown in Figure 4. The image size is 30 μm wide and 100 nm gray scale. The AFM images show the particles of TCNQ on the surfaces. The particles are uniformly distributed on the surfaces and the size is of the order of 1 μm in length. The morphology of the deposited particles changes slightly with the concentration. The number of the particles increases as the concentration increases, but the size is almost independent of the concentration.

The bearing analysis provides a method of plotting and analyzing the histogram of surface height over a sample. A surface area and a volume above a certain height are calculated using the standard NanoScope III software.[62] A successful analysis of deposited species can be made for the use of substrates having atomically smooth surfaces.[59−61] Since the bearing analysis is very sensitive to the curvature of the image plane, a third-order polynomial plane fit was used to account for the sample tilt and a slight curvature that results from coupling between the z and the $x-y$ piezoelectric positioners. The main peak at 0 nm in the histogram represents the surface height distribution and its width (full width at half-maximum: W) is a good measure of the surface roughness.[59−61] If the peak has a Gaussian shape with a standard deviation σ, W corresponds to 2.36σ and most (>95%) areas are in the $2W$ region between $-W$ and W. We define the bearing volume (V) as the volume in the bearing curve in this $2W$ region. A difference in the bearing volumes between a deposited and undoped surface is the volume of deposited very small particles present near the surface. The volume of the large particles can be directly obtained from integration of the bearing area curve above a height of W.

The surface heights of the TCNQ-deposited films from 1.03 and 0.11 mg mL^{-1} solutions distribute in a wider range (W = 4.41 and 3.35 nm, respectively) than that of the undoped film (W = 3.20 nm) because of a contribution from surface roughening and/or very small (a few nanometers height) surface reaction products of TCNQ. Much of W, in fact, may be due to roughening rather than particle deposition. For convenience, the increase of W is considered as if it is due to the presence of the small particles on the surface. The heights of the large deposited particles from 1.03 and 0.11 mg mL^{-1} solutions distribute over 70 and 40 nm, respectively. The histogram of the TCNQ-deposited film from 1.03 mg mL^{-1} solution is separated at above 4.41 nm (indicated by the marker) from the center of the surface distribution, and it gives the volumes of the deposited large and small TCNQ particles to be 2.51 and 1.23 μm^3, respectively. The histogram of the TCNQ-deposited film from 0.11 mg mL^{-1} solution is separated at above 3.35 nm from the center of the surface distribution, and it gives the volumes of the large and small TCNQ particles to be 1.23 and 0.39 μm^3, respectively. It has been shown that the surface morphology or roughness of the oxidized atomically smooth Al films does not change upon the doping with the solvent (CH_3CN). The values of Rms, W, and V of the solvent-doped surfaces agree with those of the undoped surfaces.[61]

The separated volumes of large and small particles of TCNQ on the surfaces deposited from various concentrations of CH_3CN solutions are shown in Figure 5 with the widths (W) of the main peaks in the bearing histograms. Uncertainties of the separated volumes and the widths are mainly caused by random experimental errors and are about 10%. The widths (W) of the deposited TCNQ from solutions less than 0.1 mg mL^{-1} agree well with that of the undoped surface (2.80 ± 0.65 nm), suggesting the presence of few small particles of TCNQ on the surfaces. The separated volumes of both the particles of TCNQ are also very small (less than 0.8 μm^3) in this concentration range. The W increases slowly as the concentration increases and becomes almost constant (about 4 nm) in the concentrations larger than 0.5 mg mL^{-1}. The increase in the W suggests the

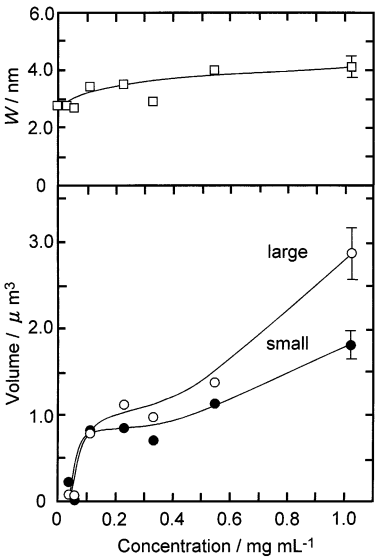

Figure 5. Bearing widths (*W*) of the bearing histograms and separated volumes of large (○) and small (•) particles of the deposited TCNQ on the atomically smooth oxidized Al films from various concentrations of CH_3CN solutions. Uncertainties for the values of *W* and both the separated volumes are 10%.

presence of small particles (about 1 nm high) on the surfaces. The volume of the large particles increases rapidly as the concentration increases, but that of the small particles increases slowly as the concentration increases. The changes in the volumes of both types of particles on the surfaces upon the concentration correlate well with the intensities of the neutral and anionic TCNQ obtained by XPS. This correlation between the separated volumes and the intensities of the surface species strongly suggests that large and small particles are the neutral and anionic TCNQ on the surface, respectively.

Adsorption State of TCNQ on Atomically Smooth Oxidized Al Films. Alumina surfaces have been studied by infrared spectroscopy and the models have been proposed.[63−66] Knözinger and Ratnasamy[66] proposed the surface models of the ideal planes of γ-Al_2O_3 and η-Al_2O_3. Though the oxygen lattice is more densely packed in γ-Al_2O_3 than in η-Al_2O_3, both aluminas have defect spinel lattices and the local ionic configurations of the $A1^{3+}$ cations are identical. Since the net charge in a stable ionic structure should be equal or nearly equal to zero, OH anions are favorable to terminate these faces. Radical anion formation of electron-acceptor molecules with high electron affinity on alumina occurs on extraordinarily coordinated OH anions on hydroxyl-rich surfaces, whereas exceptionally coordinated O^{2-} ions play the role of the donor sites on more strongly dehydroxylated surfaces.[65] TCNQ and tetracyanoethylene (TCNE) interact with donor sites on the surfaces and produce anion radicals which can be quantitatively measured by electron spin resonance (ESR). They have been used as probe molecules for the detection of donor sites on oxide surfaces.[65]

Surface-oxidized aluminum and magnesium have long served as models for catalytic oxides. Their surface models are much easier to define than conventional high surface area powders.[67−70] The vibrational spectra of TCNQ adsorbed on alumina surfaces of Al/Al_2O_3/TCNQ/Pb tunneling junctions have been measured by IETS.[51−54] The tunneling junctions were prepared by vacuum evaporation following an oxidation of Al at room temperature, giving rough surfaces as shown in our papers.[56,57,61] The tunneling spectra show that TCNQ is adsorbed predominantly as the monoanion formed from a surface reaction on the alumina,[51−54] disagreeing with the present result. However, this discrepancy can be well understood from the consideration of the morphology of the adsorbed TCNQ and the sensitivity of IETS. The present study shows that TCNQ is adsorbed onto the oxidized Al films as both a uniform film on a nanometer scale and micrometer-sized particles. The volumes of the deposited TCNQ in the thin uniform films and the large particles are obtained separately through the bearing analysis. We believe that TCNQ is predominantly in the anionic state in the thin films, while it exists in the neutral state in the large particles. Tunneling barriers thicker than a few nanometers have negligible transmission probability and thus do not contribute to the IETS.[51−54] The tunneling spectrum is mainly coming from the very thin uniform films of $TCNQ^{x-}$. On the other hand, XPS probes all the material within the analytical depth (a few tens of nanometers) of the surface and thus XPS signal is heavily weighted toward the larger particles of $TCNQ^0$. The present study clearly shows that the morphology of TCNQ on the oxide surface must be considered in order to interpret its adsorbed state obtained by any spectroscopy. The present study also shows that atomically smooth Al films are suitable and useful for such a study.

We can conclude that TCNQ is adsorbed onto the oxidized Al films as both a uniform film of anions on a nanometer scale and micrometer-sized particles with the height of a few tenth nanometer of neutral molecules. It is thought that TCNQ interacts with donor sites on the alumina to produce the anion radical ($TCNQ^{x-}$) and is adsorbed on Lewis-acid sites (Al^+) on the surfaces. Neutral TCNQ is present as multilayers over the $TCNQ^{x-}$. Both the XPS characterization and AFM morphology observation of the deposited TCNQ on the surfaces provide clear information on the adsorption mechanism.

Conclusion

Atomically smooth oxidized Al films enabled us to study the adsorption state and morphology of TCNQ deposited from acetonitrile solutions onto the oxide surfaces. The XPS study showed that TCNQ is adsorbed onto the oxide surfaces in both an ionized and neutral state. The AFM study showed that TCNQ is adsorbed as both a uniform film on a nanometer scale and micrometer-sized particles on the surfaces. The effective volumes of the two types of surface species can be obtained separately from the bearing analysis. The similarity for the dependence of both the volumes of the deposited TCNQ and that of the intensities of the ionized and neutral TCNQ on the solution concentration showed that the thin uniform film results predominantly from corrosion of the oxide surface by the TCNQ anion formation reaction and the large particles are identified as microcrystallites of neutral TCNQ. The discrepancy in the results obtained by IETS and XPS can be understood by the morphology of the adsorbed TCNQ on the alumina surfaces and differences in the spectroscopic sensitivities. We can also demonstrate the usefulness and importance of the atomically smooth Al films in modern surface science.

Acknowledgment. We thank Professor K. W. Hipps of Washington State University for his valuable comments. The present study was partially supported by Shimadzu Science and Technology Foundation and the Light Metal Educational Foundation.

References and Notes

(1) Melby, L. R.; Harder, R. J.; Hertler, W. R.; Mahler, W.; Benson, R. E.; Mochel, W. E. *J. Am. Chem. Soc.* **1962**, *84*, 3374.
(2) Torrance, J. B. *Acc. Chem. Res.* **1979**, *12*, 79.

(3) *Molecular Metals*; Hatfield, W. E., Ed.; Plenum Press: New York, 1979.
(4) Simon, J.; André, J.-J. *Molecular Semiconductors*; Springer-Verlag: Berlin, 1985.
(5) Potember, R. S.; Poehler, T. O.; Cowan, D. O. *Appl. Phys. Lett*. **1979**, *34*, 405.
(6) Potember, R. S.; Poehler, T. O.; Rappa, A.; Cowan, D. O.; Bloch, A. N. *J. Am. Chem. Soc*. **1980**, *102*, 3659.
(7) Kamitsos, E. I.; Tzinis, C. H.; Risen, W. M. *Solid State Commun*. **1982**, *42*, 561.
(8) Potember, R. S.; Poehler, T. O.; Rappa, A.; Cowan, D. O.; Bloch, A. N. *Synth. Met*. **1982**, *4*, 371.
(9) Potember, R. S.; Poehler, T. O.; Benson, R. C. *Appl. Phys. Lett*. **1982**, *41*, 548.
(10) Kamitsos, E. I.; Risen, W. M. *Solid State Commun*. **1983**, *45*, 165.
(11) Benson, R. C.; Hoffman, R. C.; Potember, R. S.; Bourkoff, E.; Poehler, T. O. *Appl. Phys. Lett*. **1983**, *42*, 855.
(12) Potember, R. S.; Hoffman, R. C.; Benson, R. C.; Poehler, T. O. *J. Phys*. **1983**, *44*, C3-1597.
(13) Poehler, T. O.; Potember, R. S.; Hoffman, R.; Benson, R. C. *Mol. Cryst. Liq. Cryst*. **1984**, *107*, 91.
(14) Kamitsos, E. I.; Risen, W. M. *Mol. Cryst. Liq. Cryst*. **1986**, *134*, 31.
(15) Kaplunov, M. G.; Timoshenko, A. V.; Borod'ko, Y. G. *Sov. J. Chem. Phys*. **1987**, *4*, 1021.
(16) Hoffman, R. C.; Potember, R. S. *Appl. Opt*. **1989**, *28*, 1417.
(17) Duan, H.; Mays, M. D.; Cowan, D. O.; Kruger, J. *Synth. Met*. **1989**, *28*, C675.
(18) Sato, C.; Wakamatsu, S.; Tadokoro, K.; Ishii, K. *J. Appl. Phys*. **1990**, *68*, 6535.
(19) Yamaguchi, S.; Viands, C. A.; Potember, R. S. *J. Vac. Sci. Technol*. **1991**, *B9*, 1129.
(20) Matsumoto, M.; Nishino, Y.; Tachibana, H.; Nakamura, T.; Kawabata, Y.; Samura, H.; Nagamura, T. *Chem. Lett*. **1991**, 1021.
(21) Hietschold, M.; Vollmann, W.; Mrwa, A.; Heilmann, A.; Hansma, P. K. *Phys. Status Solidi* **1992**, *(a)131*, 59.
(22) Hoagland, J. J.; Wang, X. D.; Hipps, K. W. *Chem. Mater*. **1993**, *5*, 54.
(23) Gu, N.; Lu, W.; Wei, Y. *Chin. Sci. Bull*. **1995**, *40*, 962.
(24) Yamaguchi, S.; Potember, R. S. *Mol. Cryst. Liq. Cryst*. **1995**, *267*, 241.
(25) Yamaguchi, S.; Potember, R. S. *Synth. Met*. **1996**, *78*, 117.
(26) Gao, H. J.; Zhang, H. X.; Xue, Z. Q.; Pang, S. J. *J. Mater. Res*. **1997**, *12*, 1942.
(27) Kamna, M. M.; Graham, T. M.; Love, J. C.; Weiss, P. S. *Surf. Sci*. **1998**, *419*, 12.
(28) Heintz, R. A.; Zhao, H.; Ouyang, X.; Grandinetti, G.; Cowen, J.; Dunbar, K. R. *Inorg. Chem.* **1999**, *38*, 144.
(29) Lijun, W.; Itaya, K. *Chin. Sci. Bull.* **2001**, *46*, 377.
(30) Ikemoto, I.; Thomas, J. M.; Kuroda, H.; Barber, M.; Hillier, I. H. *Mol. Cryst. Liq. Cryst.* **1972**, *18*, 87.
(31) Ikemoto, I.; Thomas, J. M.; Kuroda, H. *Farady Discuss. Chem. Soc.* **1972**, *54*, 208.
(32) Ikemoto, I.; Thomas, J. M.; Kuroda, H. *Bull. Chem. Soc. Jpn.* **1973**, *46*, 2237.
(33) Aarons, L. J.; Barber, M.; Connor, J. A.; Guest, M. F.; Hillier, I. H.; Ikemoto, I.; Thomas, J. M.; Kuroda, H. *J. Chem. Soc., Faraday Trans. 2* **1973**, *69*, 270.
(34) Grobman, W. D.; Pollak, R. A.; Eastman, D. E.; Maas, E. T.; Scott, B. A. *Phys. Rev. Lett.* **1974**, *32*, 534.
(35) Grobman, W. D.; Silverman, B. D. *Solid State Commun.* **1976**, *19*, 319.
(36) Kaplunov, M. G.; Shulga, Y. M.; Pokhodnya, K. I.; Borodko, Y. G. *Phys. Status Solidi (b)* **1976**, *73*, 335.
(37) Potember, R. S.; Poehler, T. O.; Cowan, D. O.; Brant, P.; Carter, F. L.; Bloch, A. N. *Chem. Scr*. **1981**, *17*, 219.
(38) Tsuchiya, S.; Seno, M. *Chem. Phys. Lett*. **1982**, *92*, 359.
(39) Tsuchiya, S. *Chem. Phys. Lett*. **1983**, *103*, 231.
(40) Lindquist, J. M.; Hemminger, J. C. *J. Phys. Chem.* **1988**, *92*, 1394.
(41) Lindquist, J. M.; Hemminger, J. C. *Chem. Mater.* **1989**, *1*, 72.
(42) Okubo, J.; Hoshi, T.; Ono, I.; Karube, K.; Kobayashi, M. *Bull. Chem. Soc. Jpn.* **1989**, *62*, 362.
(43) Giergiel, J.; Wells, S. K.; Land, T. A.; Hemminger, J. C. *Surf. Sci.* **1991**, *255*, 31.
(44) Wells, S. K.; Giergiel, J.; Land, T. A.; Lindquist, J. M.; Hemminger, J. C. *Surf. Sci.* **1991**, *257*, 129.
(45) Patterson, T.; Pankow, J.; Armstrong, N. R. *Langmuir* **1991**, *7*, 3160.
(46) Arena, A.; Di Marco, G.; Giorgi, R.; Mezzasalma, A. M.; Patanè, S.; Saitta, G. *Surf. Interface Anal.* **1994**, *22*, 511.
(47) Arena, A.; Mezzasalma, A. M.; Patanè, S.; Saitta, G. *J. Mater. Res.* **1997**, *12*, 1693.
(48) Iwamoto, H.; Higo, M.; Kamata, S. *Adv. X-ray Chem. Anal. Jpn.* **1997**, *28*, 85.
(49) Arena, A.; Patanè, S.; Saitta, G. *Nuovo Cim. D* **1998**, *20*, 907.
(50) Long, G.; Willett, R. D. *Inorg. Chim. Acta* **2001**, *313*, 1.
(51) Simonsen, M. G.; Coleman, R. V. *Phys. Rev.* **1973**, *B8*, 5875.
(52) Korman, C. S.; Coleman, R. V. *Phys. Rev.* **1977**, *B15*, 1877.
(53) Cooper, J. R.; Ivezic, T.; Zoric, I. *J. Phys.* **1982**, *C30*, L397.
(54) Hipps, K. W.; Mazur, U. *Rev. Sci. Instrum.* **1984**, *55*, 1120.
(55) Erley, W.; Ibach, H. *Surf. Sci.* **1986**, *178*, 565.
(56) Higo, M.; Lu. X.; Mazur, U.; Hipps, K. W. *Chem. Lett.* **1997**, 709.
(57) Higo, M.; Lu. X.; Mazur, U.; Hipps, K. W. *Langmuir* **1997**, *13*, 6176.
(58) Kurawaki, J.; Kusumoto, Y.; Higo, M. In *Fourier Transform Spectroscopy*; Itoh, K., Tasumi, M., Eds.; Waseda University Press: Tokyo, 1999; pp 363−364.
(59) Higo, M.; Lu. X.; Mazur, U.; Hipps, K. W. *Chem. Lett.* **1999**, 679.
(60) Higo, M.; Yoshidome, T.; Ozono, Y. *Chem. Lett.* **2000**, 1254.
(61) Higo, M.; Lu. X.; Mazur, U.; Hipps, K. W. *Thin Solid Films* **2001**, *384*, 90.
(62) *NanoScope® Command Reference Manual*; Digital Instruments, Inc.: Santa Barbara, CA 93103, 1994; Chapter 12.
(63) Peri, J. B. *J. Phys. Chem.* **1965**, *69*, 220.
(64) Tsyganenko, A. A.; Filimonov, V. N. *J. Mol. Struct.* **1973**, *19*, 579.
(65) Knözinger, H. *Adv. Catal*. **1976**, *25*, 184.
(66) Knözinger, H.; Ratnasamy, P. *Catal. Rev. Sci. Eng*. **1978**, *17*, 31.
(67) Hansma, P. K.; Hickson, D. A.; Schwarz, J. A. *J. Catal*. **1977**, *48*, 237.
(68) Bowser, W. M.; Weinberg, W. H. *Surf. Sci*. **1977**, *64*, 377.
(69) Evans, H. E.; Bowser, W. M.; Weinberg, W. H. *App. Surf. Sci*. **1980**, *5*, 258.
(70) Kroeker, R. M.; Hansma, P. K. *Catal. Rev. Sci. Eng*. **1981**, *23*, 553.